XLVI CILAMCE
VITÓRIA - ES - BRAZIL - 2025
XLVI IBERO-LATIN AMERICAN CONGRESS ON COMPUTATIONAL METHODS IN ENGINEERING

A Workflow for Wellbore Closure in Salt Formations Using Chronos: From Laboratory Testing to Numerical Simulation

Nelson Inoue[1], Sergio A. B. da Fontoura[1], Eugênio da Silva[1,3], Victor M. A. Meléndez[1], Yang Zhi[2], Constantino Nino[2], Breno Tebaldi[2], Abraão Cavalcante[2]

[1]*Group of Technology in Energy and Petroleum, Dept. of Civil and Environmental Engineering, Pontifical Catholic University of Rio de Janeiro PUC-Rio*
Rua Marques de São Vicente 225, 22451-900, Gávea, Rio de Janeiro - RJ, Brazil
inoue@puc-rio.br, fontoura@puc-rio.br, eugeniosilva@puc-rio.br, victor_me@puc-rio.br
[2]*CNOOC Petroleum Brasil Ltda*
Edifício Rio Sul, 3505, Rua Lauro Müller, 116, 22290-160, Botafogo, Rio de Janeiro - RJ, Brazil
yang.zhi@cnoocbrasil.com, constantino.nino@cnoocbrasil.com, breno.tebaldi@cnoocbrasil.com, Ext-abraao.cavalcante@cnoocbrasil.com
[3]*Rio de Janeiro State University-UERJ.*
Av. Manuel Caldeira de Alvarenga, 1203, 23070-200, Campo Grande, Rio de Janeiro - RJ, Brazil

Abstract. This study presents a workflow for simulating wellbore closure in salt formations, combining experimental testing, creep law calibration, and numerical simulation using the finite element program *Chronos*. Laboratory creep tests on halite from the Starks Dome (USA) characterized time-dependent deformation under varying stress and temperature conditions. A two-step calibration procedure, deterministic and stochastic optimization, was applied to a power-law creep model to determine its constitutive parameters. The creep law was implemented in *Chronos*, a GPU-accelerated finite element program for long-term salt creep analysis. Time-dependent equations were solved using explicit integration and a strain-hardening formulation to account for stress and temperature variations. Plane strain simulations were benchmarked against *Abaqus*, showing excellent agreement in wellbore closure and stress evolution, confirming *Chronos'* reliability for predicting salt creep behavior in subsalt drilling.

Keywords: wellbore closure, creep, finite element, *Chronos*, and *Abaqus*.

1 Introduction

Drilling oil wells through thick salt layers, such as those found in Brazil's offshore pre-salt reservoirs, presents major challenges due to the salt's time-dependent deformation (creep). When a wellbore is drilled, the stress equilibrium within the salt formation is disturbed, leading to progressive deformation that causes wellbore wall closure (Melo and Fontoura [1]) and casing integrity problems (Braga et al. [2]). Understanding and predicting this creep behavior is essential for safe and cost-effective well design.

To address this issue, the Group of Technology in Energy and Petroleum (GTEP/PUC-Rio) developed a workflow combining laboratory testing, creep law calibration, and finite element simulation of wellbore closure. Long-term triaxial creep tests on halite under controlled stress, temperature, and pressure provided data for calibrating a power-law creep model through hybrid deterministic–stochastic optimization. A GPU-accelerated finite element program, *Chronos*, has been developed for geomechanical analysis of time-dependent materials.

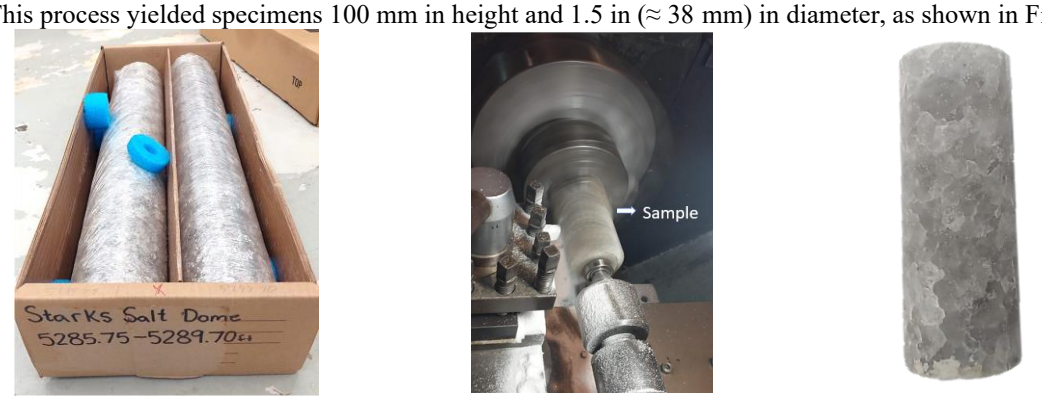
This development represents a significant step toward technological independence and scientific transparency in salt engineering modeling. It combines laboratory testing, constitutive calibration, and advanced finite element simulation within a unified workflow. Moreover, the in-house development of *Chronos*, a GPU-accelerated finite element program, provides flexibility for implementing new creep laws and numerical algorithms (contact

formulation). This open and extensible architecture enables the continuous evolution of the software to address the specific challenges of salt-related well problems in the Brazilian pre-salt context.

2 Creep tests

2.1 Halite samples and specimen preparation

In our experimental program, we tested a halite sample from the Starks Dome, Calcasieu Parish, Louisiana, USA. The halite was characterized by a density of 2.20 g/cm³ and an unconfined compressive strength (UCS) of 17.85 MPa. Figure 1(a) shows the halite as received, in the form of cylindrical cores with a diameter of 4 in (≈ 102 mm) and a length of 60 cm. The salt cylinders were subsequently cut and machined on a lathe, as shown in Fig. 1(b). This process yielded specimens 100 mm in height and 1.5 in (≈ 38 mm) in diameter, as shown in Fig. 1(c).



(a) (b) (c)

Figure 1. Photograph of the salt sample preparation steps.

2.2 Triaxial creep cells

The GTEP/PUC-Rio laboratory team developed four servo-controlled triaxial creep cells designed to perform long-term tests on evaporitic rocks and shales. These systems allow the measurement of creep strains under constant load and temperature conditions over time. One of the testing units is shown in Fig. 2(a). Each apparatus consists of a stainless-steel pressure vessel equipped with a hydraulic servo-controlled piston at its base, which provides precise axial loading, while the confining pressure is independently regulated by a servo-controlled intensifier. Figure 2(b) provides a detailed view of the instrumentation setup, showing the axial LVDTs mounted around the specimen. Three of the systems have an axial load capacity of 1000 kN, a confining pressure limit of 60 MPa, sample heating capability up to 120 °C, and a maximum axial displacement of 12.7 mm. The fourth cell differs in its higher capacity, allowing axial loads up to 1500 kN and confining pressures up to 100 MPa.



(a) (b)

Figure 2. Photograph of the (a) triaxial creep cell and (b) a view of the instrumentation setup.

2.3 Experimental test results

An experimental program consisting of nine constant-stress creep tests was conducted. The tests were performed under a confining pressure (σ_2) of 17 MPa, with axial stress differences ($\Delta\sigma$) of 5, 10, 15, and 20 MPa, and temperatures of 28°C, 50°C, and 80°C. The objective of this experimental program was to evaluate the creep behavior of the salt under constant axial stress difference and temperature, generating time-dependent strain curves to determine the parameters of a power-law through a calibration.

Figure 3 presents the total strain–time curves obtained from the experimental program. The longest test lasted 22 days, while the tests conducted at higher temperatures were limited by the maximum strain capacity of the creep testing apparatus. The creep strain was determined by subtracting the elastic component from the total strain. The elastic strain corresponds to the instantaneous deformation produced by the applied axial stress difference.

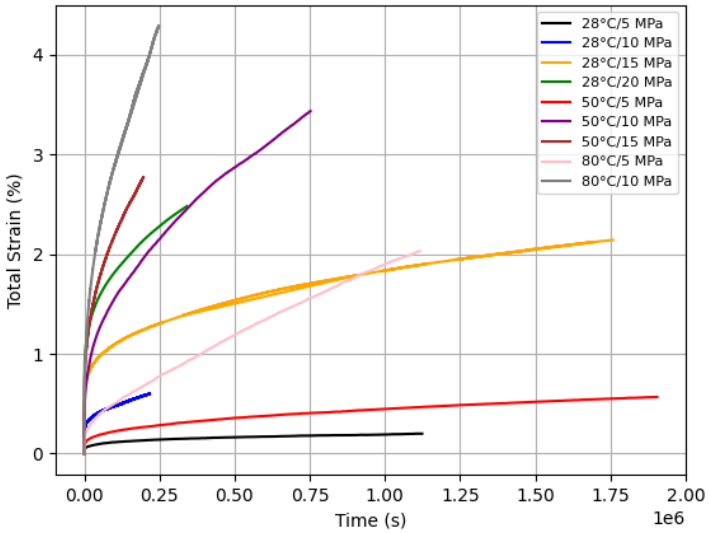


Figure 3. Total strain–time curves from the test matrix.

3 Two-step calibration process of power law

In this section, the steps involved in the calibration process of the power-law model (eq. (1)) are presented. The procedure was developed and implemented in the Python programming language, and the corresponding methodology is discussed below.

$$\varepsilon^{cr} = A \cdot t^n \cdot \Delta\sigma^m \cdot T^p \tag{1}$$

The calibration of a power law consists of determining the material parameters that best reproduce the experimental creep response, typically the coefficient A, time exponent n, stress exponent m, and temperature exponent p, so that the computed strain–time curves match the laboratory data. This process is essential for accurately describing the time-dependent deformation behavior of materials such as halite under different stress and temperature conditions.

The proposed calibration framework integrates deterministic and stochastic optimization approaches to estimate the parameters of the power-law creep equation. The stochastic stage, based on genetic algorithms, is used to refine and enhance the results obtained from the conventional deterministic calibration, leading to improved agreement between simulated and experimental creep curves. The process is fully automated, and the input data consist of creep curves obtained under different axial stress differences and temperatures, provided as Microsoft Excel files.

3.1 Deterministic calibration

The deterministic calibration procedure proposed by Hansen and Mellegard [3] consists of four main steps to determine the parameters of the power-law creep equation. First, the stress difference exponent (m) is obtained by performing linear regressions of log ε^{cr} (creep strain) versus log $\Delta\sigma$ (stress difference) at constant temperatures and evaluating the time point at which the exponent becomes stable. Next, the temperature exponent (p) is determined using a similar approach, plotting log ε^{cr} against log T (temperature) for different stress differences at the same reference time. The time exponent (n) is then derived as the average value from individual creep tests, representing the rate of strain accumulation with time. Finally, the coefficient (A) is calculated from the experimental data using the previously determined exponents, completing the parameter set of the power-law model that governs the creep behavior of the material. The power-law equation, expressed in terms of the parameters obtained from the deterministic calibration, is presented in eq. (2).

$$\varepsilon^{cr} = 1.7800\ 10^{-8} \cdot t^{0,4355} \cdot \Delta\sigma^{2,1188} \cdot T^{2,1777} \tag{2}$$

3.2 Stochastic calibration

The stochastic calibration process extends the deterministic procedure by incorporating genetic algorithms to improve the fitting of the power-law creep model. In this framework, all four parameters of the equation (m, p, n, and A) are evaluated using both deterministic and stochastic approaches. The deterministic stage provides initial estimates that preserve the physical meaning of the parameters, while the stochastic stage refines these values through genetic optimization to achieve a closer match between the simulated and experimental creep curves.

The implementation was carried out using PyGAD, a free and open-source Python library designed for genetic algorithm optimization. In this implementation, the power-law equation (eq. (1)) was embedded within the objective function (fitness_func). The gene_space parameter defines the admissible ranges for each variable. The calibration minimizes the mean absolute error between the experimental and predicted creep strains, resulting in improved fitting accuracy while maintaining physically consistent parameters. The power-law equation obtained after refinement using the genetic algorithm is presented in eq. (3).

$$\varepsilon^{cr} = 3.1792\ 10^{-9} \cdot t^{0.5167} \cdot \Delta\sigma^{1.9025} \cdot T^{2,2890} \tag{3}$$

The equations are expressed in terms of the following units: time (s), stress (MPa), and temperature (°C).

4 Chronos finite element program

The finite element program *Chronos* has been developed to simulate the long-term creep behavior of salt, aiming to advance the understanding of time-dependent deformation processes that are critical for wellbore stability and casing integrity in subsalt drilling. A three-dimensional viscoelastic formulation has been implemented in *Chronos*, assuming (i) material isotropy, (ii) coaxiality between the creep-strain-rate tensor and the deviatoric stress tensor (eq. (4)), and (iii) isochoric behavior, meaning that creep does not produce a change in volumetric strain (eq. (5)).

$$\dot{\varepsilon}_{ij}^{f} = k \cdot s_{ij} \tag{4}$$

$$\Delta\varepsilon_{V}^{cr} = \varepsilon_{x}^{cr} + \varepsilon_{y}^{cr} + \varepsilon_{z}^{cr} = 0 \tag{5}$$

Considering hypotheses (ii) and (iii), and following the mathematical developments presented in Costa [4] and Gravina [5], the invariant scalar k can be expressed as:

$$k = \frac{3}{2} \cdot \frac{\dot{\varepsilon}_{e}^{f}}{\sigma_{e}} \tag{6}$$

Substituting this expression into eq. (3), we obtain:

$$\dot{\varepsilon}_{ij}^{f} = \frac{3}{2} \cdot \frac{\dot{\varepsilon}_{e}^{f}}{\sigma_{e}} \cdot s_{ij} \tag{7}$$

where σ_e denotes the effective (or equivalent) stress, and $\dot{\varepsilon}_e^f$ is effective creep strain rate, given respectively by.

$$\sigma_e = \sqrt{\frac{3}{2}} \cdot \left(s_x^2 + s_y^2 + s_z^2 + 2\tau_{xy}^2 + 2\tau_{yz}^2 + 2\tau_{zx}^2\right)^{\frac{1}{2}} \tag{8}$$

$$\dot{\varepsilon}_e^f = \sqrt{\frac{2}{3}} \cdot \left(\dot{\varepsilon}_x^{f\,2} + \dot{\varepsilon}_y^{f\,2} + \dot{\varepsilon}_z^{f\,2} + 2\dot{\varepsilon}_{xy}^{f\ 2} + 2\dot{\varepsilon}_{yz}^{f\ 2} + 2\dot{\varepsilon}_{zx}^{f\ 2}\right)^{\frac{1}{2}} \tag{9}$$

where s_{ij} are the components of the deviatoric stress tensor.

An explicit integration algorithm has been implemented to update the state variables, such as creep strain, directly from known values at the current time step, without the need for iterative solvers. In this approach, the evolution equations (e.g., creep laws) are integrated using the current stress and material state to compute the updated response at the next time increment. Because each step depends only on previously computed quantities, explicit schemes are computationally efficient and straightforward to implement. However, they generally require small time steps to maintain numerical stability and accuracy, as explicit integration methods are conditionally stable with respect to time.

Classical empirical creep laws, such as the power law, were derived from laboratory tests conducted under constant uniaxial stress and temperature, effectively capturing time-dependent deformation in simple conditions. However, in real engineering applications, especially in finite element analyses, the stress state within materials is typically multiaxial and varies with time due to complex boundary conditions, load histories, and nonlinear material or geometric effects. Under these circumstances, traditional creep formulations become inadequate because they assume constant stress and cannot represent the influence of changing stress paths.

To overcome these limitations, the strain-hardening method was employed. This approach reformulates the creep law so that the material response depends on the accumulated creep strain rather than elapsed time alone. By doing so, it captures the effects of evolving stress states and loading histories, allowing accurate prediction of creep behavior in situations where stress and temperature vary during the simulation.

Thus, the increment of effective creep strain between two-time steps, t_n and t_{n+1}, for each element, is calculated as:

$$\Delta\varepsilon_e^f = A \cdot T^b \{\sigma_e^a(t_n)[t_{n+1} - \lambda(t_n)]^c - \sigma_e^a(t_{n-1})[t_n - \lambda(t_{n-1})]^c\} \tag{10}$$

The parameter λ, which ensures continuity of the creep strain curve under varying stress and temperature, is computed as:

$$\lambda(t_n) = t_n - \left\{[t_n - \lambda(t_{n-1})]^c \cdot \left(\frac{T_{n-1}}{T_n}\right)^b \cdot \left(\frac{\sigma_{n-1}}{\sigma_n}\right)^a\right\}^{1/c} \tag{11}$$

The complete mathematical development leading to Equations (10) and (11) is available in Costa [4] and Gravina [5].

5 Chronos results of creep simulation

To validate the implementation, a plane strain simulation was performed to evaluate the wellbore closure in a halite formation. The numerical results of displacement and stress obtained with *Chronos* were compared against those from *Abaqus*, a well-established commercial finite element program widely used in the oil and gas industry for salt creep analyses. The close agreement between both solutions confirms the reliability and accuracy of *Chronos* for geomechanical analyses of wellbore behavior in salt formations.

5.1 Well construction phases

Chronos has been designed to simulate the entire wellbore construction process, which currently includes the geostatic initialization, drilling, and creep phases. This implementation enables a stepwise representation of stress redistribution and deformation during wellbore creation within a realistic geomechanical workflow.

The simulation process is structured as follows:

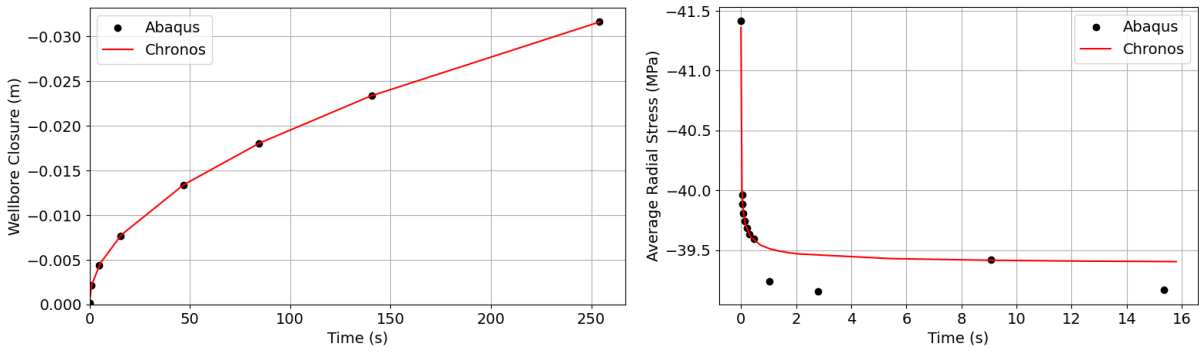
(i) Initial conditions. The simulation begins by defining appropriate boundary conditions and assigning the initial in-situ stress field to the domain, representing the pre-drilling geostatic equilibrium of the subsurface.

(ii) Geostatic step. A geostatic initialization is performed to ensure that the system is in static equilibrium, meaning that internal stresses are balanced by the applied boundary loads. In this case, the in-situ stresses are defined as $\sigma_V = \sigma_H = \sigma_h = -53.37$ MPa, corresponding to a pre-salt scenario typical of the Santos Basin and a true vertical depth (TVD) of 3000 meters.
(iii) Drilling step. The displacement constraints (boundary conditions) previously applied to the wellbore wall are removed, simulating the excavation process associated with drilling. This removal allows the surrounding formation to deform in response to the stress redistribution induced by the creation of the wellbore. Subsequently, a mud pressure of $p_w = 35.25$ MPa is applied to the wellbore wall to represent the hydrostatic pressure exerted by the drilling fluid column.
(iv) Creep step. After the drilling phase, the creep step is performed to simulate the time-dependent deformation of the salt formation surrounding the wellbore. During this stage, the mechanical response of the material evolves under the combined effects of the redistributed stress, temperature, and applied mud pressure. The simulation captures the gradual development of creep strain and stress relaxation over time, allowing the evaluation of long-term wellbore closure.

5.2 Simulation results

The results of wellbore closure and stress evolution over time are presented to analyze the wellbore's geomechanical behavior and to evaluate the accuracy of the *Chronos* results against *Abaqus*, which was served as the benchmark reference.

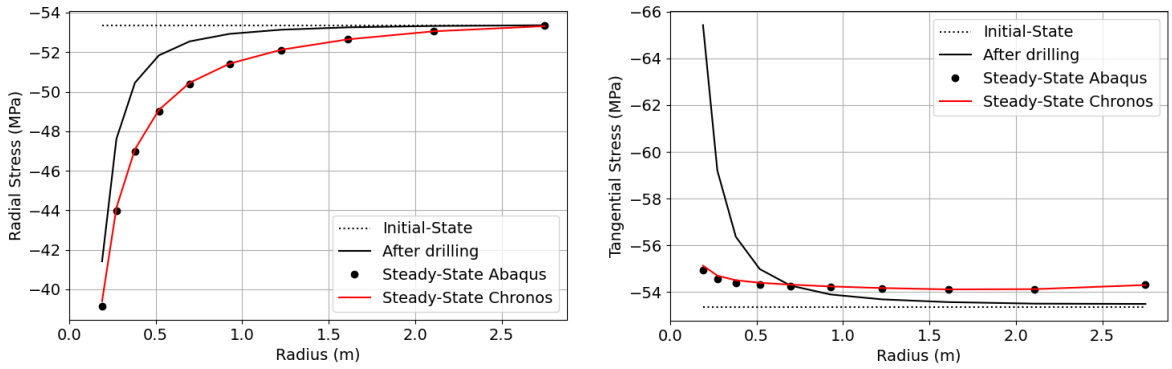
Figure 4(a) shows the evolution of wellbore closure over time, considering a 9 5/8″ casing. The annular space is 0.033 m, indicating that the rock salt comes into contact with the casing approximately 250 s (4 min 10 s) after drilling. It is important to note that such rapid closure may lead to stuck pipe conditions during drilling operations. Regarding numerical accuracy, *Chronos* shows excellent agreement with *Abaqus*, demonstrating a nearly perfect match between both results. Figure 4(b) shows that the material reaches its "long-term strength" or "flow strength" at approximately 16 seconds. This indicates that the stress relaxation process does not continue indefinitely but instead stabilizes once a steady equilibrium state is achieved. The *Abaqus* results, plotted as black dots, exhibit small fluctuations caused by the time increment size. In contrast, the *Chronos* result (red line) shows smoother behavior due to the use of smaller time increments.



(a) (b)

Figure 4. (a) Wellbore closure over time; and (b) average radial stress reaching the steady state.

Figure 5(a) and (b) show the results of radial and tangential stresses, respectively, for three conditions: the initial state, after drilling, and at steady state. After this stage, stress relaxation ceases, and only minor variations in the stress distribution are observed. The stress relaxation phase occurs very rapidly, after which creep deformation continues with practically no further change in stress over time, similar to the behavior observed in a conventional creep test. It was observed that both the radial and tangential stresses show excellent agreement between *Chronos* and *Abaqus*, with the steady-state condition accurately predicted and maintained constant over time by *Chronos*.



(a) (b)

Figure 5. Evolution of (a) radial and (b) tangential stresses along the radius over time.

6 Conclusions

The study established a complete experimental–numerical workflow to model salt creep and its implications for wellbore closure. Laboratory creep tests on halite provided reliable data for calibrating time-dependent constitutive models. A two-step calibration method, integrating deterministic regression and stochastic optimization via genetic algorithms, enhanced model fitting and ensured physical consistency of parameters. The *Chronos* finite element program, featuring explicit integration and strain-hardening formulations, successfully reproduced *Abaqus* benchmark results, validating its robustness and accuracy. Overall, the workflow offers a reliable and efficient workflow for predicting long-term wellbore closure in salt engineering.

Acknowledgements. The authors gratefully acknowledge the financial support provided by CNOOC Petroleum Brasil Ltda and the Brazilian National Agency for Petroleum, Natural Gas and Biofuels (ANP) through the R&D program regulated by ANP Resolution nº 50/2015. The authors also thank the Group of Technology in Energy and Petroleum (GTEP/PUC-Rio) for the laboratory infrastructure and technical support that made this research possible.

Authorship statement. The authors hereby confirm that they are the sole liable persons responsible for the authorship of this work, and that all material that has been herein included as part of the present paper is either the property (and authorship) of the authors, or has the permission of the owners to be included here.

References

[1] D. D. E. F. Melo and S. A. B. Fontoura, "Wellbore Closure in Salt Section with Consideration of Primary Creep." In: ISRM IX Latin American Rock Mechanics Symposium (LARMS 2022), International Society for Rock Mechanics and Rock Engineering, October 16–19, 2022. Paper ISRM-LARMS-2022-45.
[2] J. J. V. Braga, D. D. E. F. Melo, S. A. B. Fontoura, and L. F. M. Almeida, "Pre-Salt Numerical Analysis in Casing Integrity Considering the Main Events During the Well Lifespan." In: 55th U.S. Rock Mechanics/Geomechanics Symposium, American Rock Mechanics Association, Houston, June 18–25, 2021. Paper ARMA-2021-1994.
[3] F. D. Hansen and K. D. Mellegard, "Creep of 50 mm diameter specimens of dome salt from Avery Island, Louisiana," Topical Report RSI-0118 (ONWI-104), 1980.
[4] A. M. da Costa. Uma aplicação de Métodos Computacionais e Princípios de Mecânica das Rochas no Projeto e Análise de Escavações Destinadas à Mineração Subterrânea. Tese (Doutorado em Engenha Civil), COPPE/Universidade Federal do Rio de Janeiro, Rio de Janeiro, RJ, 1984.
[5] C. C. Gravina. Simulação numérica do comportamento mecânico do sal em poços de petróleo. Dissertação (Mestrado em Engenharia Mecânica), Universidade Estadual de Campinas, Faculdade de Engenharia Mecânica, Campinas, SP, 1997.